Cenozoic Relative Movements of Greenland and North America by Closure of the North Atlantic-arctic Plate Circuit: the Labrador Sea, Davis Strait and Baffin Bay

Annabel Causer (annabel.causer.2017@live.rhul.ac.uk)
Royal Holloway, University of London
Graeme Eagles
Alfred Wegener Institute, Helmholtz Centre for Polar and Marine Research
Lucía Pérez-Díaz
Department of Earth Sciences, Oxford University
Jürgen Adam
Royal Holloway, University of London

Article

Keywords: plate divergence, Cenozoic relative movements, North Atlantic-Arctic plate circuit, Labrador Sea, Davis Strait, Baffin Bay, Greenland and North America

Posted Date: August 26th, 2021

DOI: https://doi.org/10.21203/rs.3.rs-840254/v1

Abstract

The processes that accommodated plate divergence between Greenland and North America are most confidently interpretable from a short-lived (61-42 Ma) sequence of magnetic isochrons in the Labrador Sea. Understanding of the preceding and following periods is impeded by the lack of clear isochrons in the basin's continent-ocean transition and axial zones. By closing the regional plate circuit, we build and interpret a detailed plate motion model for Greenland and North America that is applicable in, but unaffected by data uncertainty from, the Labrador Sea, Davis Strait, and Baffin Bay. Among our findings, we show the Labrador Sea initially opened during a ~8.3-16.5 Myr-long period of focused extension culminating in continental breakup no earlier than 74-72 Ma, and experienced a ~80° change in spreading direction around 56 Ma. We describe some possible implications for the accommodation of strain prior to continental breakup and during extreme spreading obliquity.

1. Introduction

A wealth of seafloor spreading data is available for most parts of the North Atlantic Ocean, but near the continental margins they become more and more difficult to justify as unequivocal signals of oceanic crustal accretion [1–5]. This problem is particularly prominent for studies of the relative motions of plates bearing Greenland and North America, which formed oceanic basins in the Labrador Sea and its smaller neighbour Baffin Bay (Figs. 1 and 2)[1,2,6,7]. From the basin margins, the earliest signs of rifting are interpreted from diverse alkaline igneous intrusions that are dated to Late Triassic or early Jurassic times[8,9]. Younger intrusions have been related to Kimmeridgian (~ 150 Ma) and Early Cretaceous (~ 140 – 133 Ma) extension[9]. Sedimentation in fault-bounded basins started in the Early Cretaceous, and gave way to regional thermal subsidence at a poorly-constrained later in the Cretaceous[10].

The majority of modern plate kinematic models for the region rely heavily on magnetic anomaly identifications from the Labrador Sea[1,2,6,7,11] (Fig. 3). The consensus from magnetic anomaly studies (e.g.[12,13]) is that steady-state seafloor spreading was certainly underway by chron C26 (59 Ma) at the latest (Figs. 2 and 3), although many authors cite a slightly older age of C27 (62 Ma; e.g.[2]). During that period, the North Atlantic region was visited by large-volume magmatism related to the Iceland Plume, whose products at the continental margins are expressed in seismic reflection data as seaward dipping reflectors (SDRs; Fig. 2;[14,15]). This event not only accompanied the onset of steady-state seafloor spreading in the Labrador Sea, it was swiftly followed at ~ 56 Ma by a fundamental change in the orientation of plate divergence related to the onset of seafloor spreading between Greenland and Eurasia[2]. The youngest consistently-identifiable magnetic reversal isochron in the Labrador Sea is C20 (42 Ma), but a broad swath of seafloor lies between it and the mid-ocean ridge. Using North Atlantic magnetic isochrons near the South Greenland Triple Junction, this seafloor can be attributed to ongoing spreading until extinction of the ridge at ~ 33 Ma[16].

Outside the Labrador Sea and the C27-C13 period, understanding is less evenly shared. Weak magnetic anomaly lineations marginward of C27 have been related to sources in thin igneous crust formed at distributed sites within broad continent-ocean transition zones (see[17–19]). It remains open to question whether such settings might produce dateable linear magnetic reversal isochrons like those over thicker (~ 7 km) standard oceanic crust and, thus, whether published interpretations of the weak anomalies as reversal isochrons as old as C33 [1,20] can be seen as reliable (~ 79 Ma; Fig. 2). Davis Strait connects the Labrador Sea and Baffin Bay regions, and is host to two large N-S trending transform faults (see, Fig. 3) which are thought to have acted as sheared continental margin segments during Paleocene and Eocene times[21–25]. The affinity of the crust in the floor of Davis Strait is uncertain[21,26,27]. To the north, wide-angle seismic profiles [23,25,28,29] and a clear extinct median valley [30] leave little doubt about the absence of continental crust in Baffin Bay. Beyond this, the basin's plate tectonic history is understood by comparison to the Labrador Sea's owing to the lack of strong linear magnetic anomaly signals [28,31,32]. This has proved difficult to reconcile with the widespread evidence for Eocene convergent tectonics in and around Baffin Bay[2,29,33,34].

Here we revisit the region's tectonic evolution by closure of its plate circuit. Using seafloor spreading data (magnetic anomaly isochrons of undisputed oceanic origin and fracture zone traces) from the North Atlantic and Arctic Ocean we produce two independent models describing 1) Eurasian–North American (EUR-NAM) plate divergence and 2) Greenland–Eurasian (GRN-EUR) divergence (Fig. 2), since as early as mid-Cretaceous times. Focusing on the late Cretaceous – Eocene time period, we generate a Greenland–North America (GRN-NAM) plate model by adding the GRN-EUR and EUR-NAM rotations (Fig. 1). In this way, we produce a framework solution for the Labrador Sea—Baffin Bay region that is insensitive to conflicting interpretations of the region's geological and geophysical data sets. Using this framework, we show that continental breakup between the North American and Eurasian plates in the Labrador Sea dates to no earlier than C33 (74 Ma). We suggest it is possible this breakup occurred when the plate boundary propagated through a set of abandoned rift basins produced during earlier Cretaceous distributed extension. Breakup was followed by the formation of broad continent-ocean transition zones until, at C27 (61 Ma), the onset of NE-SW-oriented oceanic accretion at a stable mid-ocean ridge. Soon after its formation, the ridge was adopted as the site of NNW-SSE-oriented divergence between the North American and Greenland plates. The ridge retained its orientation in spite of the large (70–80°) accompanying change in plate divergence direction. We suggest it is possible that, in response, large normal faults along the median valley started to act in oblique slip, unlike at active mid ocean ridges of similar length where spreading obliquity nowhere exceeds 45°. Our model suggests very little oceanic crust would have been generated in Davis Strait in pre-Paleocene times, and that afterwards it became a site of transpressional deformation. Well-known compressional structures in Baffin Bay are a result NW-SE oriented compressive phase during the Middle to Late Eocene (C21 – C13; 46–33 Ma) that followed the cessation of plate divergence at C21 (46 Ma).

2. Results

2.1 Eurasia – North America plate divergence

The solution for the EUR-NAM plate pair is shown in Supplementary Figure S1a-c, as sets of visual fits of isochron picks and synthetic ridge-crest flowlines rotated to target great circle segments and fracture zone traces respectively. Including outliers, the technique reduces misfits to means and standard

deviations of 1.40 km and 13.03 km for magnetic isochron data and 0.06 km and 4.22 km for fracture zone data. Large misfits in the magnetic data are geographically evenly spread, with the exception of small higher-misfit clusters associated with older isochron data around the Labrador Sea triple junction between the North American, Eurasian and Greenland plates (Fig. 1). Poorly fitting segments of flowlines are associated with small asymmetrical features resulting from ridge-jump or propagation episodes. If outliers are neglected under the assumption that the misfits should adopt standard Gaussian distributions, then the mean values of isochron and fracture zone data misfits reduce to 1.05 km and 0.20 km, and their standard deviations to 3.81 km and 3.38 km, respectively.

Supplementary Figure S2 shows the locations of 25 new finite rotation poles and their associated 95% confidence ellipses, describing the relative divergence of Eurasia and North America since the Late Cretaceous (C34; 84 Ma). The locations illustrate two distinct trends in plate motion, with a marked shift from NW to S/SSW-migrating poles centred on C13 (33 Ma, Eocene-Oligocene boundary). These trends are in good agreement with previous studies in the North Atlantic and Arctic Oceans, but also benefit from the greater stability and smoothness that our inversion scheme can deliver, compared to others. Confidence ellipses were calculated using the rotation parameters and covariance matrices in Supplementary Table S1. Confidence regions are largest for the younger isochrons, reflecting the small-angle rotations over long continuous segments.

2.2 Greenland – Eurasia plate divergence

Our GRN-EUR model uses data from the Iceland and Irminger Basins in the period between breakup (which we approximate using small sets of picks from the conjugate shelf edges, labelled GES, and preliminarily date to chron C25; 57 Ma) and C13 (Paleocene – Eocene). The model is summarized in Supplementary Figure S3. It extends to chron C13 (33 Ma) in order to enable our subsequent closure of the plate circuit to include the time at which seafloor spreading in the Labrador Sea is suggested to have ceased. Including outliers, the mean values of magnetic isochrons and fracture zones misfits are 0.15 km and − 0.20 km, and their standard deviations are 15.09 km and 4.99 km, respectively. The greatest misfits to synthetic flowlines are located between chrons C13 and C20, where the signals of fracture zones in gravity data [35] become weaker and harder to interpret with confidence. Neglecting outliers by assuming Gaussian distributions of misfits for magnetic isochron and fracture zone data, mean misfits reduce to 0.30 km and 1.51 km, and standard deviations to 8.65 km and 3.67 km, respectively.

Supplementary Figure S4 and Table S2 detail the rotation poles and 95% confidence ellipses generated from the rotation parameters and misfit statistics described above. Between Paleocene and Eocene times (GES – C21; ~57–46 Ma) poles move progressively southward, and then migrate towards the east until C13 (33 Ma), consistent with the behaviour observed in previous models for the region (Supplementary Fig. S4).

2.3 Greenland – North America plate divergence

The summation of rotation parameters and combination of their associated covariances generates a set of rotation parameters and covariances for Paleocene to Eocene (GES-C13) movement in the Labrador Sea. The resulting rotation poles, and 95% confidence ellipses calculated from the covariance matrices, are shown in Fig. 5. The covariance matrices are presented in Table 1 along with a comparison to other models. All show how the finite rotation poles in the GRN-NAM plate model migrate towards the southwest from Paleocene times until the Eocene-Oligocene boundary (GES – C33; ~57–33 Ma).

Prior to GES, with Greenland moving as part of a rigid Eurasian plate, our manipulation of the EUR-NAM model yields a set of finite rotations for times ranging back to the Late Cretaceous (C34 – GES; 84–57 Ma). The estimated uncertainty regions are somewhat larger than those for GES and later times, reflecting the fact that these rotations are generated by the combination of three rotations each (see Methods section), but even at this level of confidence the rotations differ starkly from those in the studies by [1,2].

Figure 5 illustrates the GRN-NAM model using a set of synthetic ridge-crest flowlines beginning at seeds distributed along the axes of the Labrador Sea's mid-ocean ridge. The synthetic flowlines closely match the lengths and orientations of fracture zone segments preserved on both flanks of the extinct mid-ocean ridge [2,6,35], suggesting that the model provides an appropriate plate kinematic context within which to understand the regional geology. More prescriptively for the level of confidence at which we can expect to do so, our circuit-based model predicts the locations of the well-known magnetic reversal isochrons C24 – C20 (53–42 Ma) in the Labrador Sea to within its corresponding 95% confidence ellipses (Fig. 5).

Immediately prior to C24, the 95% confidence ellipses of the GES marker lie inboard of the C25 (57 Ma) isochron in the Labrador Sea, without enveloping picks of it (Fig. 5). The model spacing between GES and C24 is around two-thirds of the real-world spacing of isochrons C24 and C25 (57.10 to 53.41 Ma) in the Labrador Sea, prompting us to revise our preliminary estimate of the age of GES from 57 Ma to around 55.9 Ma. Continental breakup between Greenland and Eurasia in the Irminger – Iceland basins thus post-dates C25, in agreement with magnetostratigraphic determination of chron C24r (54–56 Ma) in the oldest drilled sediments of the Irminger Basin[36].

The revised date for GES invalidates the assumption that our GRN-EUR and NAM-EUR rotations for GES and C25 are time equivalents that can be summed in the plate circuit. Figure 4 illustrates that the effect of this is nonetheless relatively insignificant; the set of pre-Eocene rotation poles calculated using a NAM-EUR rotation interpolated to 55.9 Ma (the revised age of GES) all lie within the corresponding 95% confidence ellipses calculated using the less accurate age for GES (black poles; Fig. 4). Flowlines calculated from the two alternative sets of pre-GES rotations in Fig. 5 show how, in the Labrador Sea, the additional error related to the mis-dating of GES is similar in size (~ 15 km) to the misfit between the GES-aged flow points and picks of the C25 isochron.

3. Discussion

3.1 Opening of the Labrador Sea

3.1.1 A precondition for continental breakup: Paleocene Labrador Sea

The NE-SW oriented pre-Eocene flowlines segments in the Labrador Sea are constrained by the EUR-NAM model at C25, C31, C33, and C34. Picks of isochron C27 (from the GFSML repository;[37]) lie close to linearly-interpolated flowpoints for their age (62 Ma), suggesting they are reliable signals of EUR-NAM seafloor spreading (Fig. 5). In contrast, Roest & Srivastava's, (1989)[1] picks of C31 and C33 lie well outside of the 95% confidence ellipses for the constrained EUR-NAM flowpoints of the same ages. This reinforces the conclusions of previous studies that the weak magnetic anomalies of the older parts of the Labrador Sea are not related to the presence of oceanic crust. Among them, Keen et al., (2018)[19] use seismic data to identify a proto-oceanic zone in the seafloor that our flowlines date to C29-C27 (65 – 62 Ma) and between C29 and the continental shelf a basement of serpentinized and exhumed mantle. Our results strongly suggest that linear magnetic anomalies in such settings are unlikely to be useful as dated plate edge isochrons for kinematic reconstructions.

Using Keen et al's., (2018)[19] findings to assume the pre-C27 seafloor comprises a transition zone of newly-created proto-oceanic crust and mechanically-exhumed mantle, the flowlines can be used to estimate an earliest possible timing of continental breakup by observing where they pass over the transition zone's landward margins. In the southern Labrador Sea, where pairs of flowlines cross the margins symmetrically, breakup in a two-plate (Eurasia-North America) setting would have occurred no earlier than the time between chrons C33 and C32 (74 – 72 Ma; late Campanian). The transition zone between the shelf edge and isochron C27, thus, seems to have formed over a period of at most 12 – 10 Myr, considerably more rapidly than suggested [2,38]. The necking zones landward of the transition zone range in width between 100 and 200 km [19]. Conservatively assuming a mean stretching factor of 2.0 and no igneous crustal addition, the formation of these zones would require plate divergence in the range 50–100 km. With rates like those shown in Fig. 7, our NAM-EUR model would have achieved this over a period of 8.3–16.5 Myr prior to breakup at 74 – 72 Ma. The focused crustal extension responsible for forming the necking zones thus seems unlikely to have started any earlier than a date in the range 90.5–80.3 Ma.

The kinematic evolution of extended continental margins has been suggested to involve high-strain episodes that culminate in continental breakup following crustal softening over the courses of much longer-enduring periods of lower strain [39]. The short period required for developing the Labrador Sea's necking zones, beginning at 90.5–80.3 Ma and ending at 74 – 72 Ma, fits the concept of rapid strain prior to breakup. Products of the preceding period of slow extensional strain date however to 140 – 100 Ma [10], leaving an unexplained gap of 9.5–19.7 Myr duration in the Labrador margin's overall strain history. Ball et al., (2013) [40] suggested a similar-length gap at the extended margin off southern Australia, and that its products might lie invisibly buried deep in the necking zone. Later, detailed analysis of Australian-Antarctic plate divergence showed the gap not only to be real, but also to have lasted considerably longer, around 80 Myr [41]. If these gaps are real, then they suggest that strain softening in distributed rift zones occurs by processes whose products, and the associated mechanical weakness, can be preserved over long periods of tectonic quiescence to be exploited for continental breakup at later times.

Rotations to GES calculated using the EUR-NAM model occur about North Pacific poles, closer to the northern part of the Labrador Sea than its southern part. Consequently, Paleocene plate divergence in the south of the Labrador Sea was ~ 5% faster than in the north. This difference does not support an interpretation of the presence of SDRs at the northern continental margins in the Labrador Sea and exhumed mantle further south [19] in terms of contrasting plate divergence and mantle upwelling rates. Furthermore, plate divergence rates calculated from the model for the time and location of SDR formation (C27; 62 Ma) are ~ 11 mma^{-1} (Fig. 7), within the global range for magma-poor margins [42,43]. These observations all suggest that the SDRs are rather products of proximity to the Iceland plume, consistent with the presence of Selandian (61 Ma) picrites along the southwest Greenland margin [10,21,44,45]. Further south in the Labrador Sea, a related effect of plume arrival seems to have been the onset of a melt flux sufficient to produce oceanic crust with a basaltic layer thickness capable of raising linear magnetic reversal anomalies. The time lag between breakup and this volcanism reinforces previous conclusions that continental breakup in the Labrador Sea was a response to far field stresses, rather than mantle plume activity [46,47].

3.1.2 Oblique slip accommodating very oblique seafloor spreading? Eocene Labrador Sea

Figure 7 shows that the rate of plate divergence in the Labrador Sea remained close to ~ 10 mma^{-1} throughout the model period. Along with the onset of Greenland plate motion at time GES (~ 55.9 Ma), however, the model shows a dramatic change in the azimuth of Labrador Sea plate divergence, which rotates anticlockwise by nearly 80°. Magnetic isochrons from before and after the rotation (C26 – C22; 59–49 Ma) show that much of the ridge crest retained its Paleocene strike despite this change, leaving it oriented strongly oblique to the new azimuth of plate divergence. Worldwide, there are no long segments of active mid-ocean ridges whose obliquity to the plate divergence azimuth exceeds 45° [48]. Studies of such active settings show that oblique slip focal mechanisms are rare, and that instead oblique ridges are populated by en echelon sets of strike-slip faults and short-lived normal faults whose strikes run approximately perpendicular to the azimuth halfway between the plate divergence azimuth and the normal to the ridge crest [49]. In the Labrador Sea after GES, the strike of such normal faults, if they developed, should have been slightly south of east, but we cannot confirm their presence with available data. Gravity anomalies, instead, suggest the presence of abyssal hills parallel to the fossil ridge crest and magnetic isochrons (Fig. 5). We consider this to leave open the possibility that large normal faults at the Labrador Sea ridge may have acted in oblique slip after GES, and that oblique slip may occur more commonly at high-obliquity spreading centres than is known from active, moderate-obliquity, examples.

Isochrons younger than C20 are absent from the flanks of the fossil median valley in the Labrador Sea. In our model, seafloor spreading rates drop slightly, but crucially, into the ultra-slow category for the first time at C20 (Fig. 7). This is consistent with the lack of clear magnetic isochrons, because ultra-slow spreading is associated with accommodation of plate divergence by mechanical, rather than igneous, processes, producing a thin and discontinuous basaltic carrier layer [50], as observed in the central region of the Labrador Sea (e.g. [51,52]). The geometry of the South Greenland Triple Junction suggests these processes may have endured until close to the Eocene – Oligocene boundary (C13; 33 Ma; [53]). Our model shows that pairs of estimated 95% confidence regions for C13-aged flow points on opposing plates do not overlap with each other (Fig. 5), suggesting extremely slow plate motion parallel to the Labrador Sea ridge axis may have continued for a short period of time after 33 Ma.

3.2 Davis Strait

Davis Strait connects the Labrador Sea to Baffin Bay. The crustal nature of its floor is uncertain from existing geological and geophysical studies (e.g. [21,26,27]). A prominent basement and seafloor high, the Davis Strait High, runs NNE along the floor of the strait. Measured parallel to the high, the strait today is around 400 km long. At first order, our whole plate flowlines in Fig. 8 show around ~ 250 km of this length to have developed since GES from the NNE-oriented component of a phase of relatively constant NNW to N-directed relative plate motion. Resolved across the high, the cross-axial component of this motion would have brought the Greenland and North American plates into convergence by around 180 km since GES. This finding of oblique convergence reinforces those of previous plate kinematic models [2,7], interpretations of geophysical and geological data [21,25,54,55], and numerical models [56]. Two features of our model (Fig. 8) may add details to these earlier conclusions. The first is to suggest that the Davis Strait oblique collision may have occurred in two stages, at GES-C22 (~ 56 – 49 Ma) and C21-C13 (46 – 33 Ma), separated by a short interval of strike-slip motion parallel to the Davis Strait High. The second is the possibility of a period of slight (< 10 km) of extension, oriented orthogonal to the axis of the Davis Strait High, following the Eocene-Oligocene transition (C13; 33 Ma).

Based on this, we attribute uplift of the Davis Strait High (Fig. 2), the development of thrust faults and folds in the Ikermiut Fault Zone where the high intersects the Greenland continental margin [57,58], and thrust faulting interpreted from seismic profiles throughout the Baffin Bay and Davis Strait areas [59] to the convergent component of a period or periods of transpression since 57 Ma. The complementary strike-slip component is recorded in onshore data by evidence for left-lateral motion within the Itilli Fault Complex east of the Davis Strait High [60].

3.3 Resolution of a convergence conundrum: Baffin Bay

Baffin Bay lacks clearly-interpretable magnetic anomaly isochrons (e.g. [25]), but like the Labrador Sea it does host a prominent extinct mid-ocean ridge [30]. Our model, shown in Fig. 9, provides a detailed new context within which to understand Baffin Bay's tectonic history with considerable confidence. Using ridge-crest flowlines, the figure depicts pre-Eocene NE-SW plate divergence, perpendicular to NW-SE striking normal faults within the bay's continental margins [34] and parallel to fracture zones identifiable from gravity data [61]. The flowlines cross onto the continental shelves close to chron C28 (63 Ma), suggesting continental breakup in Baffin Bay occurred 7–9 Myr later than in the Labrador Sea. This is consistent with the idea that the North American-Eurasian plate boundary propagated northwards through the region during late Cretaceous and earliest Paleogene times. Following the onset of Greenland Plate motion at GES (56 Ma), the model shows a period of N-S to NNW-SSE oriented plate divergence that lasts until the middle Eocene (C21; 46 Ma). This orientation is parallel to the set of fracture zones and large transfer faults that gravity data show arrayed around the basin's extinct mid-ocean ridge [61] (Fig. 9). After C21, the model shows NW- to W-oriented motion that is overall obliquely convergent to the trend of the extinct ridge crest. The implied plate collision at 46 Ma suggests that plate divergence at the mid-ocean ridge in Baffin Bay ceased ~ 13 million years earlier than previously understood.

Existing plate models struggle to explain compression along the northern margin of Baffin Bay contemporaneous with the action of a divergent plate boundary in the basin [29,33,34]. Some, such as that of [2] accommodate the contrast by the introduction of a large strike-slip fault zone continuing onshore into Arctic Canada along strike from the "Bower Fracture Zone", Fig. 9). To date, there is little evidence for such a strike-slip zone from on-shore geology [62]. Instead of these complexities, our model requires compression to post-date plate divergence in Baffin Bay. This is consistent with the seismic observation of NW trending compressional structures very close to the extinct spreading ridge [33], but also of middle Eocene (post-C21, 46 Ma) inversion structures in the Melville Graben (Knutz and Gregersen, 2012) or the hiatus observed in the Hellefisk-1 well [64]. The wide geographical distribution of these observations suggests that plate convergence after C21 was accommodated regionally in Baffin Bay and its margins, rather than focused on the inactivated ridge crest.

4. Methods

To investigate controversies surrounding magnetic anomalies in the Labrador Sea and Paleocene – Eocene relative motions there and in the Davis Strait and Baffin Bay, we generate and manipulate two plate kinematic models for the EUR-NAM and GRN-EUR plate pairs. Using the inversion technique of (Nankivell, 1997)[65], as described by Eagles, (2004)[66] and Livermore et al., (2005)[67], we resolved the locations of twenty-five finite rotation poles and angles of rotation about them for EUR-NAM and six for GRN-EUR, by minimizing the misfits of sets of small and great circle segments to the locations of fracture zone traces and magnetic anomaly data in the North Atlantic Ocean (Supplementary Figures S1a-c and S3). These two models serve as constraints for a third, describing the movements of GRN-NAM. This third model, unlike others currently available, is completely independent of interpretations of geological and geophysical data from those small oceanic basins, and can therefore be used as a framework within to evaluate those interpretations with confidence.

4.1 Data Set

Our data set is composed of fracture zone traces and oceanic magnetic anomaly picks (Supplementary Figures S1 a-c and S3). We picked fracture zone traces south of 80°N from the vertical gradient of high resolution satellite altimetry data [35], and those in the Arctic region (80 to 90°N) from ship-borne gravity anomaly data [68]. In the Irminger Basin we include two early Eocene NW-SE trending fracture zones from gravity data [35] which are thought to be representative of the basement structure during early plate divergence, e.g. [69]. Picks were interpolated at 10 km intervals along their traces.

Magnetic reversal isochron picks for both the EUR-NAM and GRN-EUR models were taken from the GSFML repository for marine magnetic identifications [37] and dated according to the [70] timescale. The EUR-NAM model isochron sequence dates back as far as C34 (84 Ma). The GRN-EUR model, which describes seafloor spreading with a later onset, is constrained by a subset of Paleocene - Eocene age picks in the same sequence (C24-C13; 54 – 33 Ma), cf. [71]. We use the post-C13 picks from these basins, which post-date independent motion of the Greenland Plate, as input for our EUR-NAM model. In order to calculate a Paleocene plate circuit solution, we include an additional, non-magnetic, isochron pick of the continental shelves (GES) in the Iceland and Irminger basins, landward of their identified SDR's [72]. Initially, GES was assigned an approximate age of C25 (57 Ma).

When compiling our data set, we excluded fracture zones and magnetic anomaly picks north of Iceland and from the Greenland – Lofoten Basins (Supplementary Figure S3). These data describe independent Paleogene motion of a plate bearing the Jan Mayen Microcontinent that was neither the Greenland nor the Eurasian plate [15], meaning they are neither suitable nor necessary for summation in our circuit to investigate the Labrador Sea.

4.2 Circuit Closure

Assuming plates are internally rigid, then the sum of the rotations describing plate motion within any given plate circuit that begins and ends with the same plate will be zero. Thus, rotations for the GRN-NAM pair can be calculated by summing those for the GRN-EUR and EUR-NAM plate pairs. Statistical confidence regions for these rotations were calculated by manipulations of the covariance matrices of the summed rotations, as detailed by [73].

Pre-GES plate divergence in the Labrador Sea can be investigated in terms of EUR-NAM plate divergence, under the assumption that Greenland would have moved as part of a rigid Eurasian plate prior to the onset of EUR-GRN divergence. In effect, the circuit is closed using a null rotation for EUR-GRN. To do this, we calculate a set of EUR-NAM rotations for periods ending with the GES rotation, when EUR-GRN motion started, and sum the results to the EUR-GRN rotation for GES to generate full finite rotations to the end of EUR-GRN plate divergence. We did this in two ways. Firstly, by assuming that GES coincides in time with C25, which enabled us to estimate confidence regions by convolution of the three sets of rotations on the peripheries of the C25 ellipse, the ellipse for the older end of the period of interest, and the GES ellipse. Secondly, we did this by assuming a more appropriate date for GES (see main text), yielding rotations without confidence regions.

Table 1

Finite rotations and covariance for the Greenland and North American plate model, derived from the North American and Eurasian, and, the Greenland and E (Iceland-Irminger Basins) plate models. Rotational parameters according to the models of [1,2] are shown. All rotations are for Greenland relative to a stationar America.

	Rotation Parameters (°)				Variance			Covariance		
Chron	Age (Ma)	Lat. (λ)	Lon. (ϕ)	Ang. (θ)	λ,λ	ϕ,ϕ	θ,θ	λ, ϕ	λ, θ	ϕ,θ
13	33.15	-71.59	140.20	0.74	503,897.06	109,775.10	262.51	-235,192.14	-11,501.23	5,3
20	42.30	-63.79	108.17	2.52	21,810,844.66	1,545,202.39	1658.41	-5,805,356.84	-190,187.76	50,
21	45.72	-61.74	102.99	3.46	21,877,103.11	817,162.73	713.62	-4,228,137.67	-124,946.97	24,
22	48.56	-61.60	86.26	3.38	9,118,980,980.64	29,922,825.47	2006.95	522,365,452.08	-4,277,993.48	-24
24	53.41	-46.21	66.64	3.67	6,154,929.38	421,551.58	682.37	161,081.81	-64,807.10	-16,
GES	57.10	-39.82	59.99	3.78	5,954,573.29	453,168.31	1119.43	1,642,684.68	-81,643.64	-22,

Other Studies

Roest & Srivastava, (1989)

Chron	Age (Ma)	Lat. (λ)	Lon. (ϕ)	Ang. (θ)
C21	45.72	-62.80	117.20	2.61
C24	53.41	-55.86	75.45	4.44
C25	57.10	-24.48	42.75	3.12

Oakey & Chalmers, (2012)

Chron	Age (Ma)	Lat. (λ)	Lon. (ϕ)	Ang
C21	45.72	-53.2	67.1	1.6
C24	53.41	-53.2	67.1	3.7
C25	57.10	-24.5	42.7	3.1

Declarations

Data Availability:

Magnetic data for this paper were obtained from the Global Seafloor Fabric and Magnetic Lineation Data Base Project [37]. High resolution gravity data (free-air) up to 80°N was obtained from [35] and ship-bourne gravity data from 80°-90°N was obtained from the Circum-Arctic mapping project [68].

Inversion models and rotational parameters for the North American – Eurasian and Greenland – Eurasian models are found in supplementary material.

Code Availability:

Necessary codes for reproducing these results are found in the depository.

Acknowledgements:

We thank COMPASS Consortium, Royal Holloway University of London for funding support. Figures were produced using the Generic Mapping Tools (GMT;[76]). We also thank Tabea Altenbernd for the provision of shape files in Figures 6, 8 and 9.

Authors' Contribution:

AC created the inversion models, drafted the original manuscript and figures. GE provided scripts to run all inversion models, discussions on results and valuable comments in improving the manuscript. LPD & JA provided important discussion and helped in revising the manuscript.

References

1. Roest, W. R. & Srivastava, S. P. Sea-floor spreading in the Labrador Sea: a new reconstruction. *Geology* **17**, 1000–1003 (1989).
2. Oakey, G. N. & Chalmers, J. A. A new model for the Paleogene motion of Greenland relative to North America: Plate reconstructions of the Davis Strait and Nares Strait regions between Canada and Greenland. *J. Geophys. Res. Solid Earth* **117**, 1–28 (2012).
3. Torsvik, T, H. *et al.* Global Plate Motion Frames : *Rev. Geophys.* **46**, 1–44 (2008).
4. Müller, R. D., Sdrolias, M., Gaina, C. & Roest, W. R. Age, spreading rates, and spreading asymmetry of the world's ocean crust. *Geochemistry, Geophys. Geosystems* **9**, 1–19 (2008).
5. Barnett-Moore, N., Hosseinpour, M. & Maus, S. Assessing discrepancies between previous plate kinematic models of Mesozoic Iberia and their constraints. *Tectonics* **35**, 1843–1862 (2016).
6. Srivastava, S. P. & Roest, W. R. Extent of oceanic crust in the Labrador Sea. *Mar. Pet. Geol.* **16**, 65–84 (1999).
7. Oakey, G. N. Cenozoic evolution and lithosphere dynamics of the Baffin Bay – Nares Strait region of Arctic Canada and Greenland. *Ph.D. thesis, Vrije University, Amsterdam, The Netherlands*. (2005).
8. Tappe, S. *et al.* Craton reactivation on the Labrador Sea margins: 40Ar/39Ar age and Sr-Nd-Hf-Pb isotope constraints from alkaline and carbonatite intrusives. *Earth Planet. Sci. Lett.* **256**, 433–454 (2007).
9. Larsen, L. M. *et al.* Tectonomagmatic events during stretching and basin formation in the Labrador Sea and the Davis Strait: Evidence from age and composition of Mesozoic to Palaeogene dyke swarms in West Greenland. *J. Geol. Soc. London.* **166**, 999–1012 (2009).
10. Dickie, K., Keen, C. E., Williams, G. L. & Dehler, S. A. Tectonostratigraphic evolution of the labrador margin, atlantic canada. *Mar. Pet. Geol.* **28**, 1663–1675 (2011).
11. Srivastava, S. P. Evolution of the Eurasian Basin and its implications to the motion of Greenland along Nares Strait. *Tectonophysics* **114**, 29–53 (1985).
12. Chalmers, J. A. New evidence on the structure of the Labrador Sea/Greenland continental margin. *J. Geol. Soc. London.* **148**, 899–908 (1991).
13. Chalmers, J. A. & Laursen, K. H. Labrador Sea: the extent of continental and oceanic crust and the timing of the onset of seafloor spreading. *Mar. Pet. Geol.* **12**, 205–217 (1995).
14. Hopper, J. R. *et al.* Continental break-up and the onset of ultraslow seafloor spreading off Flemish Cap on the Newfoundland rifted margin. *Geology* **32**, 93–96 (2004).
15. Gaina, C., Nasuti, A., Kimbell, G. S. & Blischke, A. Break-up and seafloor spreading domains in the NE Atlantic. *Geol. Soc. Spec. Publ.* **447**, 393–417 (2017).
16. Kristoffersen, Y. & Talwani, M. Extinct triple junction south of Greenland and the Tertiary motion of Greenland relative to North America. *Bull. Geol. Soc. Am.* **88**, 1037–1049 (1977).
17. Gillard, M., Manatschal, G. & Autin, J. How can asymmetric detachment faults generate symmetric Ocean Continent Transitions? *Terra Nov.* **28**, 27–34 (2016).
18. Stanton, N. *et al.* Geophysical fingerprints of hyper-extended, exhumed and embryonic oceanic domains: the example from the Iberia–Newfoundland rifted margins. *Mar. Geophys. Res.* **37**, 185–205 (2016).
19. Keen, C. E., Dickie, K. & Dafoe, L. T. Structural characteristics of the ocean-continent transition along the rifted continental margin, offshore central Labrador. *Mar. Pet. Geol.* **89**, 443–463 (2018).
20. Srivastava, S. P. & Tapscott, C. R. Plate kinematics of the North Atlantic. *Geol. North Am.* **M**, 379–404 (1986).
21. Chalmers, J. A. & Pulvertaft, T. C. R. Development of the continental margins of the Labrador Sea: A review. *Geol. Soc. Spec. Publ.* **187**, 77–105 (2001).
22. Funck, T., Jackson, H. R., Louden, K. E. & Klingelhöfer, F. Seismic study of the transform-rifted margin in Davis Strait between Baffin Island (Canada) and Greenland: What happens when a plume meets a transform. *J. Geophys. Res. Solid Earth* **112**, 1–22 (2007).
23. Funck, T., Gohl, K., Damm, V. & Heyde, I. Tectonic evolution of southern Baffin Bay and Davis Strait: Results from a seismic refraction transect between Canada and Greenland. *J. Geophys. Res. Solid Earth* **117**, 1–24 (2012).
24. Hosseinpour, M., Müller, R. D., Williams, S. E. & Whittaker, J. M. Full-fit reconstruction of the labrador sea and baffin bay. *Solid Earth* **4**, 461–479 (2013).
25. Suckro, S. K. *et al.* The crustal structure of southern Baffin Bay: Implications from a seismic refraction experiment. *Geophys. J. Int.* **190**, 37–58 (2012).
26. Srivastava, S. P. *Davis Strait: Structures, Origin and Evolution. Structure and Development of the Greenland-Scotland Ridge. Nato Conference Series (IV Marine Science),* **8**, (1983).
27. Tucholke, B. E. & Fry, V. A. Basement Structure and Sediment Distribution in Northwest Atlantic Ocean. *Am. Assoc. Pet. Geol. Bull.* **69**, 2077–2097 (1985).
28. Reid, I. & Jackson, H. R. Crustal structure of northern Baffin Bay: Seismic refraction results and tectonic implications. *J. Geophys. Res. B Solid Earth* **102**, 523–542 (1997).
29. Altenbernd, T., Jokat, W., Heyde, I. & Damm, V. A crustal model for northern Melville Bay, Baffin Bay. *AGU J. Geophys. Res. Solid Earth* **120**, 1195–1209 (2014).

30. MacLeod, S. J., Williams, S. E., Matthews, K. J., Müller, R. D. & Qin, X. A global review and digital database of large-scale extinct spreading centers. *Geosphere* **13**, 911–949 (2017).
31. Keen, C. E. & Barrett, D. L. Seismic Refraction Studies in Baffin Bay: An Example of a Developing Ocean Basin. *Geophys. J. R. Astron. Soc.* **30**, 253–271 (1972).
32. Keen, C., Keen, M. J., Ross, D. I. & Lack, M. Baffin Bay: Small Ocean Basin Formed by Sea-Floor Spreading. *Am. Assoc. Pet. Geol. Bull.* **58**, 1089–1108 (1974).
33. Harrison, J. C., Brent, T. A. & Oakey, G. N. Chapter 40: Baffin Fan and its inverted rift system of Arctic eastern Canada: Stratigraphy, tectonics and petroleum resource potential. *Geol. Soc. Mem.* **35**, 595–626 (2011).
34. Gregersen, U., Hopper, J. R. & Knutz, P. C. Basin seismic stratigraphy and aspects of prospectivity in the NE Baffin Bay, Northwest Greenland. *Mar. Pet. Geol.* **46**, 1–18 (2013).
35. Sandwell, D. T., Müller, R. D., Smith, W. H. F., Garcia, E. & Francis, R. New global marine gravity model from CryoSat-2 and Jason-1 reveals buried tectonic structure. *Science (80-.).* **346**, 65–67 (2014).
36. Ali, J. R. & Vandamme, D. Eocene-Miocene magnetostratigraphy of the southeast Greenland Margin and western Irminger Basin. *Proc. Ocean Drill. Progr. Sci. Results* **152**, 253–257 (1998).
37. Seton, M. *et al.* Community infrastructure and repository for marine magnetic identifications. *Geochemistry, Geophys. Geosystems* **15**, 1629–1641 (2014).
38. Chalmers, J. A. The continental margin off southern Greenland: Along-strike transition from an amagmatic to a volcanic margin. *J. Geol. Soc. London.* **154**, 571–576 (1997).
39. Brune, S., Williams, S. E., Butterworth, N. P. & Müller, R. D. Abrupt plate accelerations shape rifted continental margins. *Nature* **536**, 201–204 (2016).
40. Ball, P., Eagles, G., Ebinger, C., McClay, K. & Totterdell, J. The spatial and temporal evolution of strain during the separation of Australia and Antarctica. *Geochemistry, Geophys. Geosystems* **14**, 2771–2799 (2013).
41. Eagles, G. A little spin in the Indian Ocean plate circuit. *Tectonophysics* **754**, 80–100 (2019).
42. Pinheiro, L. M., Whitmarsh, R. B. & Miles, P. R. The ocean-continental boundary off the western continental continental margin of Iberia - II. Crustal structure in the Tagus Abyssal Plain. *Geophys. J. Int.* **109**, 106–124 (1992).
43. Sauter, D. *et al.* Oceanic basement roughness alongside magma-poor rifted margins: Insight into initial seafloor spreading. *Geophys. J. Int.* **212**, 900–915 (2018).
44. Srivastava, S. P. Evolution of the Labrador Sea and its bearing on the early evolution of the North Atlantic. *Geophys. J. R. Astron. Soc.* **52**, 313–357 (1978).
45. Graham, D. W. *et al.* Helium isotope composition of the early Iceland mantle plume inferred from the Tertiary picrites of West Greenland. *Earth Planet. Sci. Lett.* **160**, 241–255 (1998).
46. Peace, A. L., Foulger, G. R., Schiffer, C. & McCaffrey, K. J. W. Evolution of labrador Sea-Baffin Bay: Plate or plume processes? *Geosci. Canada* **44**, 91–102 (2017).
47. Clarke, D. B. & Beutel, E. K. Davis Strait Paleocene picrites: Products of a plume or plates? *Earth-Science Rev.* **206**, 102770 (2020).
48. Seton, M. *et al.* A Global Data Set of Present-Day Oceanic Crustal Age and Seafloor Spreading Parameters. *Geochemistry, Geophys. Geosystems* **21**, 1–15 (2020).
49. Fournier, M. & Petit, C. Oblique rifting at oceanic ridges: Relationship between spreading and stretching directions from earthquake focal mechanisms. *J. Struct. Geol.* **29**, 201–208 (2007).
50. Dick, J.B, H., Lin, J. & Schouten. An ultraslow-spreading class of ocean ridge. *Nature* **426**, 405–412 (2003).
51. Srivastava, S. P. & Keen, C. E. A deep seismic reflection profile across the extince Mid-Labrador Sea spreading centre. *Tectonics* **14**, 372–389 (1995).
52. Delescluse, M., Funck, T., Dehler, S. A., Louden, K. E. & Watremez, L. The oceanic crustal structure at the extinct, slow to ultraslow Labrador Sea spreading center. *J. Geophys. Res. Solid Earth* **120**, 5249–5272 (2015).
53. Oakey, G. N. & Stephenson, R. Crustal structure of the Innuitian region of Arctic Canada and Greenland from gravity modelling: Implications for the Palaeogene Eurekan orogen. *Geophys. J. Int.* **173**, 1039–1063 (2008).
54. Peace, A. *et al.* The role of pre-existing structures during rifting, continental breakup and transform system development, offshore West Greenland. *Basin Res.* **30**, 373–394 (2018).
55. Gion, A. M., Williams, S. E. & Müller, R. D. A reconstruction of the Eurekan Orogeny incorporating deformation constraints. *Tectonics* **36**, 304–320 (2017).
56. Farangitakis, G. P., Heron, P. J., McCaffrey, K. J. W., van Hunen, J. & Kalnins, L. M. The impact of oblique inheritance and changes in relative plate motion on the development of rift-transform systems. *Earth Planet. Sci. Lett.* **541**, 116277 (2020).
57. Dalhoff, F. *et al.* Continental crust in the Davis Strait: New evidence from seabed sampling. *Geol. Surv. Denmark Greenl. Bull.* 33–36 (2006). doi:10.34194/geusb.v10.4901
58. Gregersen, U. & Bidstrup, T. Structures and hydrocarbon prospectivity in the northern Davis Strait area, offshore West Greenland. *Pet. Geosci.* **14**, 151–166 (2008).
59. Gregersen, U., Knutz, P. C., Nøhr-Hansen, H., Sheldon, E. & Hopper, J. R. Tectonostratigraphy and evolution of the west Greenland continental margin. *Bull. Geol. Soc. Denmark* **67**, 1–21 (2019).
60. Sørensen, E. V. *et al.* Inversion structures as potential petroleum exploration targets on Nuussuaq and northern Disko, onshore west Greenland. *Geol. Surv. Denmark Greenl. Bull.* **38**, 45–48 (2017).

61. Chalmers, J. A. & Oakey, G. N. No Title. in *Cretacous - Palaeogene development of the Labrador Sea and Davis Strait, poster A0048 presented at Annual assembly European Geoscience Union, Vienna* (2007).
62. Denyszyn, S. W., Halls, H. C., Davis, D. W. & Evans, D. A. D. Paleomagnetism and U-Pb geochronology of Franklin dykes in high arctic Canada and Greenland: A revised age and paleomagnetic pole constraining block rotations in the Nares Strait region. *Can. J. Earth Sci.* **46**, 689–705 (2009).
63. C. Knutz, P., G. Gregersen, U. & R. Hopper, J. Late Paleogene Submarine Fans in Baffin Bay and North-West Greenland. *74th EAGE Conf. Exhib. Inc. Eur. 2012* (2012). doi:10.3997/2214-4609.20148203
64. Nøhr-Hansen, H. *Dinoflagellate cyst stratigraphy of the Palaeogene strata from the Hellefisk-1, Ikermiut-1, Kangâmiut-1, Nukik-1, Nukik-2 and Qulleq-1 wells, offshore West Greenland. Marine and Petroleum Geology* **20**, (2003).
65. Nankivell, A. P. Tectonic evolution of the Southern Ocean between Antarctica, South America and Africa over the past 84 Ma. *PhD thesis* (1997).
66. Eagles, G. Tectonic evolution of the Antarctic-Phoenix plate system since 15 Ma. *Earth Planet. Sci. Lett.* **217**, 97–109 (2004).
67. Livermore, R., Nankivell, A., Eagles, G. & Morris, P. Paleogene opening of Drake Passage. *Earth Planet. Sci. Lett.* **236**, 459–470 (2005).
68. Gaina, C. *et al.* Chapter 3: Circum-Arctic mapping project: New magnetic and gravity anomaly maps of the Arctic. *Geol. Soc. Mem.* **35**, 39–48 (2011).
69. Louden, K. E., Tucholke, B. E. & Oakey, G. N. Regional anomalies of sediment thickness, basement depth and isostatic crustal thickness in the North Atlantic Ocean. *Earth Planet. Sci. Lett.* **224**, 193–211 (2004).
70. Gradstein, F. M., Ogg, J. G. *The Geological Time Scale*. **2**, (Elsevier, 2012).
71. Gaina, C., Roest, W. R. & Müller, R. D. Late Cretaceous-Cenozoic deformation of Northeast Asia. *Earth Planet. Sci. Lett.* **197**, 273–286 (2002).
72. Larsen, H. C. & Saunders, A. D. Tectonism and volcanism at the southeast Greenland rifted margin: a record of plume impact and later continental rupture. *Proc. Ocean Drill. Progr. Sci. Results* **152**, 503–533 (1998).
73. Chang, J., Stock, T. . & Molnar, P. The rotation group in plate tectonics and the representation of uncertainties of plate reconstructions. *Geophys. J. Int.* **101**, 649–661 (1990).
74. Piepjohn, K., Von Gosen, W. & Tessensohn, F. The Eurekan deformation in the Arctic: An outline. *J. Geol. Soc. London.* **173**, 1007–1024 (2016).
75. Foulger, G. R. *et al.* The Iceland Microcontinent and a continental Greenland-Iceland-Faroe Ridge. *Earth-Science Rev.* **206**, 102926 (2020).
76. Wessel, P. & Smith, W. H. F. Free software helps map and display data. *Eos, Trans. Am. Geophys. Union* **72**, 441–446 (1991).

Figures

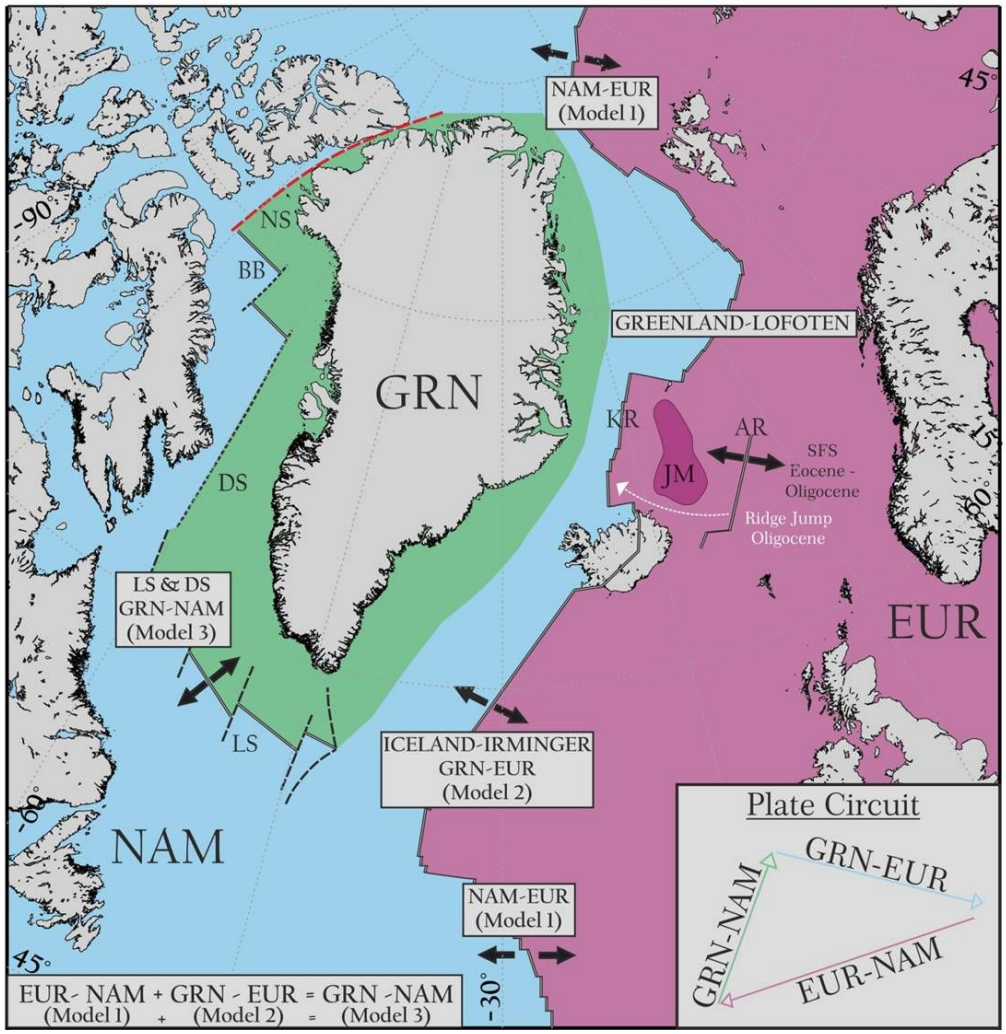

Figure 1

Present day configuration of the Greenland, North America and Eurasian Plates. Black and white lines are spreading centres. Black dashed lines are fracture zones and black solid lines are transform faults. The red dashed line marks the plate boundary between Greenland and North America along the Canadian Arctic. Abbreviations as follows: AR; Aegir Ridge, BB; Baffin Bay, DS; Davis Strait EUR; Eurasia, GRN; Greenland, JM; Jan Mayen Microcontinent, KR; Kolbeinsey Ridge, LS; Labrador Sea, NAM; North America, SFS; Seafloor Spreading.

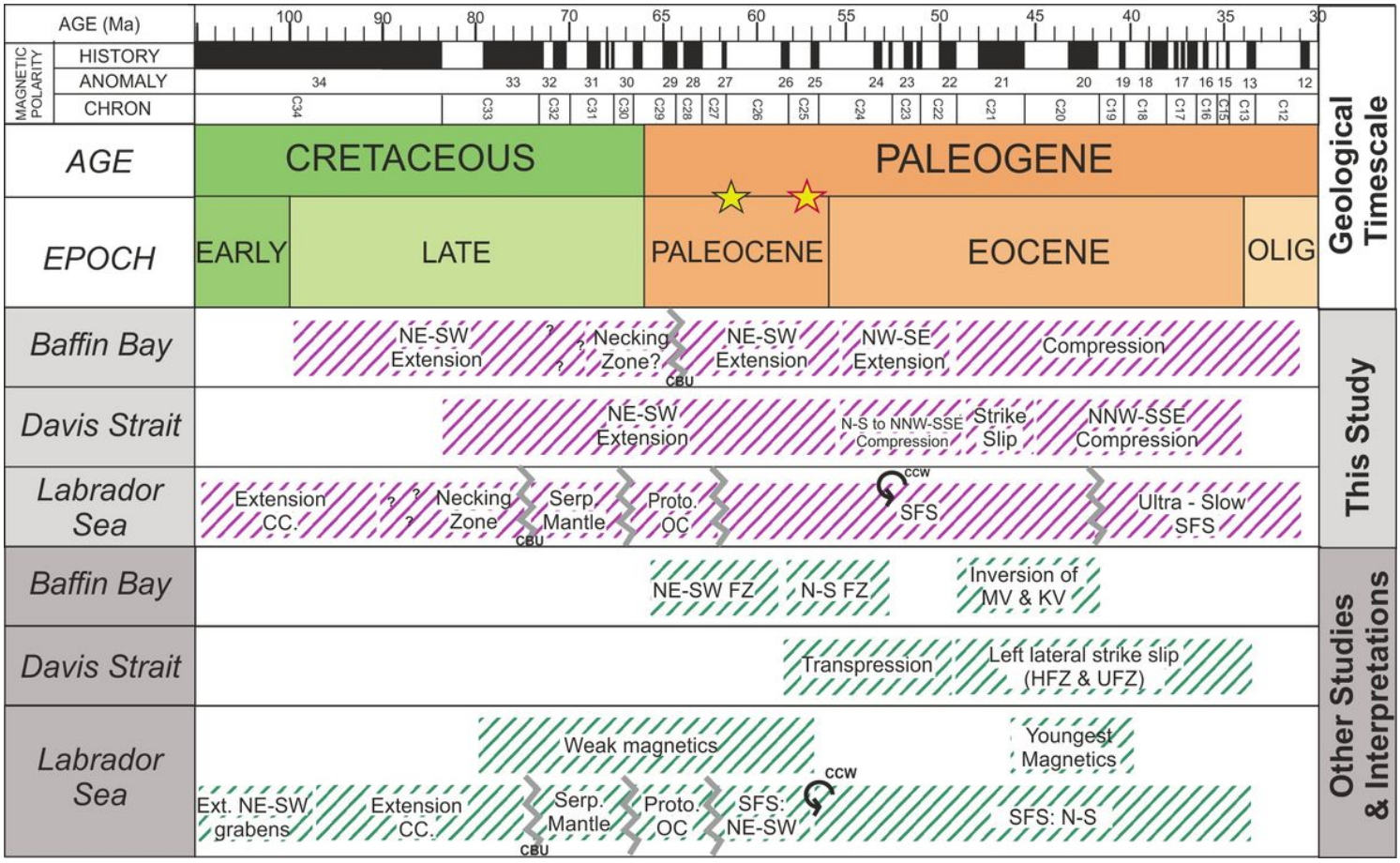

Figure 2

Chronostratigraphic chart showing the main events. Yellow and black star represent the North Atlantic Igneous Province, and yellow and red star seaward dipping reflectors in the Irminger Basin.

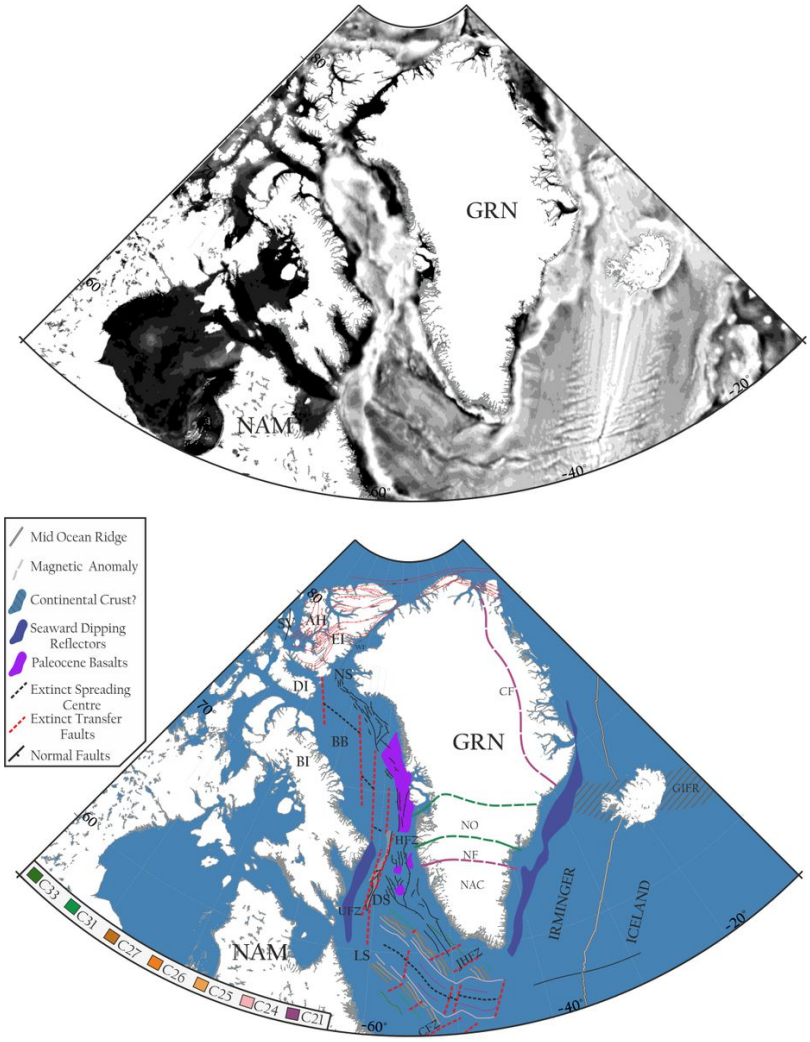

Figure 3

Present day configuration of Greenland and North America, showing vertical gravity gradient data 35,68. Providing an overview of present day and extinct spreading centres, magnetic anomalies, extensional structures and compressional structures. Seaward dipping reflectors from 54, Labrador Sea and Baffin Bay data from 1, Davis Strait and Baffin Bay normal faults from 2. Red lines show main compressional features from the Eurekan Orogenic event in Arctic Canada, from 74. Orogenic fronts according to 75. Abbreviations as follows: AH; Axel Heiberg, BB; Baffin Bay, BI; Baffin Island, CF; Caladonian Front, CFZ; Cartwright Fracture Zone, DI; Devon Island, DS; Davis Strait, EI; Ellesmere Island, GIFR; Greenland – Iceland – Faroe Ridge, JHFZ; Julian-Haab Fracture Zone, LS; Labrador Sea, NAC; North American Craton, NF; Nagssogtoqidian Orogen, NF; Nagssogtoqidian Front, SV; Sverdrup Basin, UFZ; Ungava Fault Zone, WF; Wegener Fault.

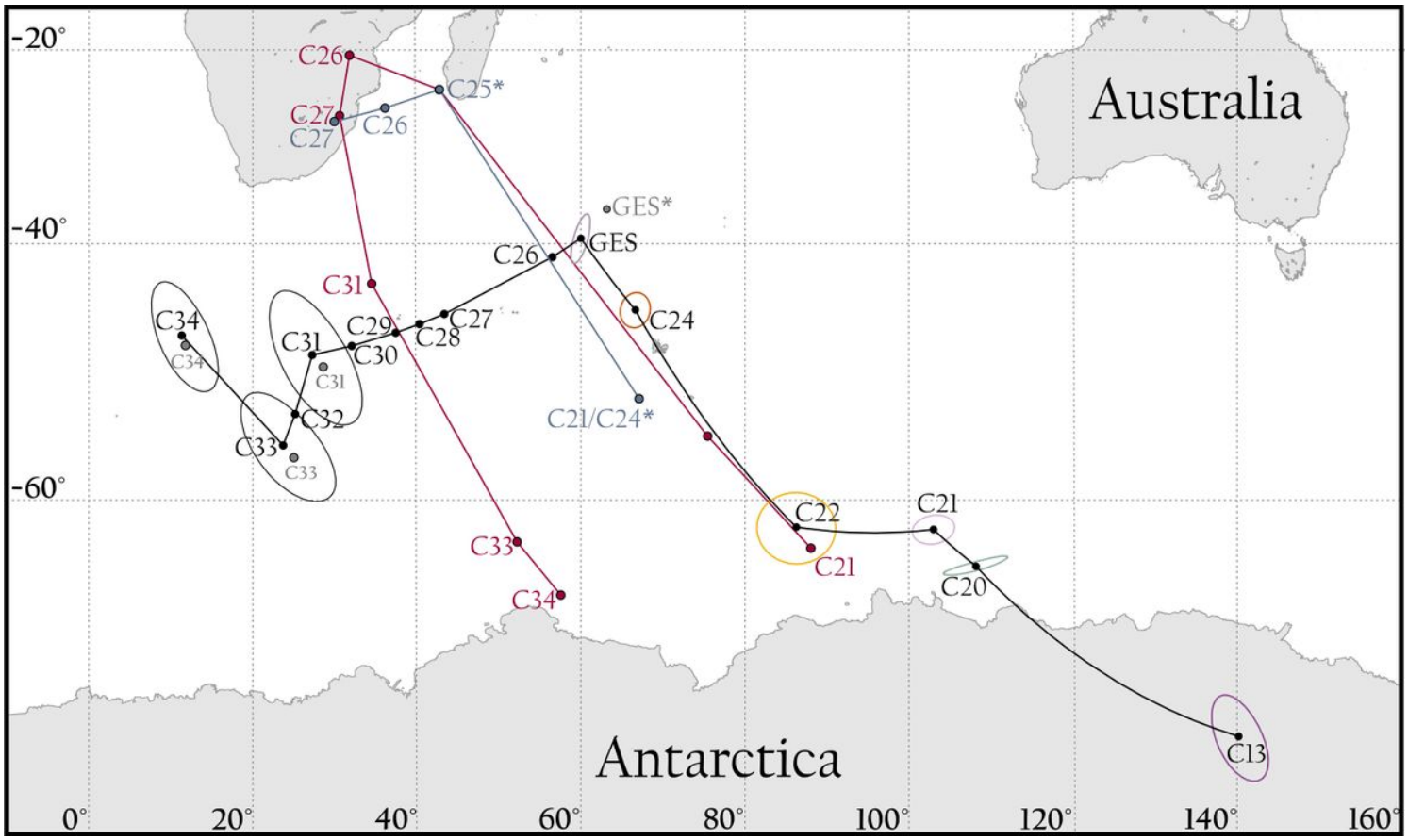

Figure 4

Finite rotational poles for the Greenland and North American plate model. Coloured confidence ellipses are combined 95% ellipses form the Eurasian and North American, and, Greenland and Eurasian plate models. Black finite rotational poles and 95% confidence ellipses are combined GES (Greenland – North America) and Eurasia and North America Plate Models. Grey GES corresponds to interpolated (55.9 Ma) rotational pole, and subsequent pre-GES grey poles are calculated using this without confidence. Red line and black points represent finite rotational poles from 1. Blue line and black points represent finite rotational poles from 2, C21/C24* shows two rotation poles in the same location. C25* represents the C25 poles of 1,2, which lie in close proximity.

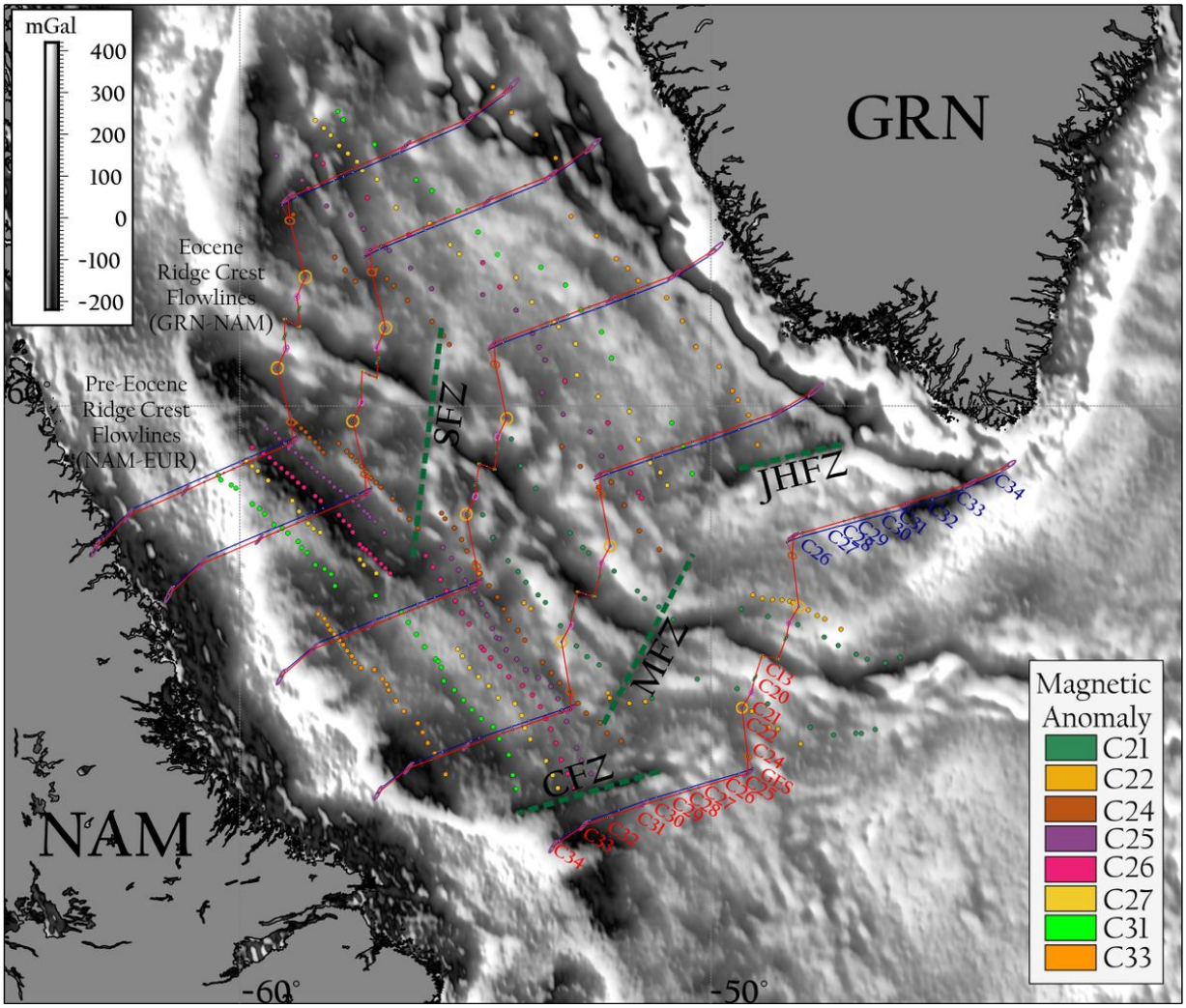

Figure 5

Plot of ridge crest flowlines from the Greenland and North America plate model, with their respective 95% confidence ellipses in the Labrador Sea (C13 – C25). Synthetic ridge-crest flowlines both originate at a common along the extinct spreading centre in the Labrador Sea. Red ridge-crest flowlines pre-GES age (55.9 Ma) calculated assuming C25 from GRN-NAM is equal to GES. Blue ridge crest flowlines pre-GES calculated assuming interpolated age of GES (lon/lat/ang; -39.951/63.184/3.67) calculated assuming an age of 56 Ma. Magnetic anomalies C24 and C25 according to GSFML; 37 , C21 and C22 71 and gravity data 35. Abbreviations as in Figure 3. Flow points for C26, C27, C28, C29, C30 and C32 are generated by interpolation to the appropriate ages.

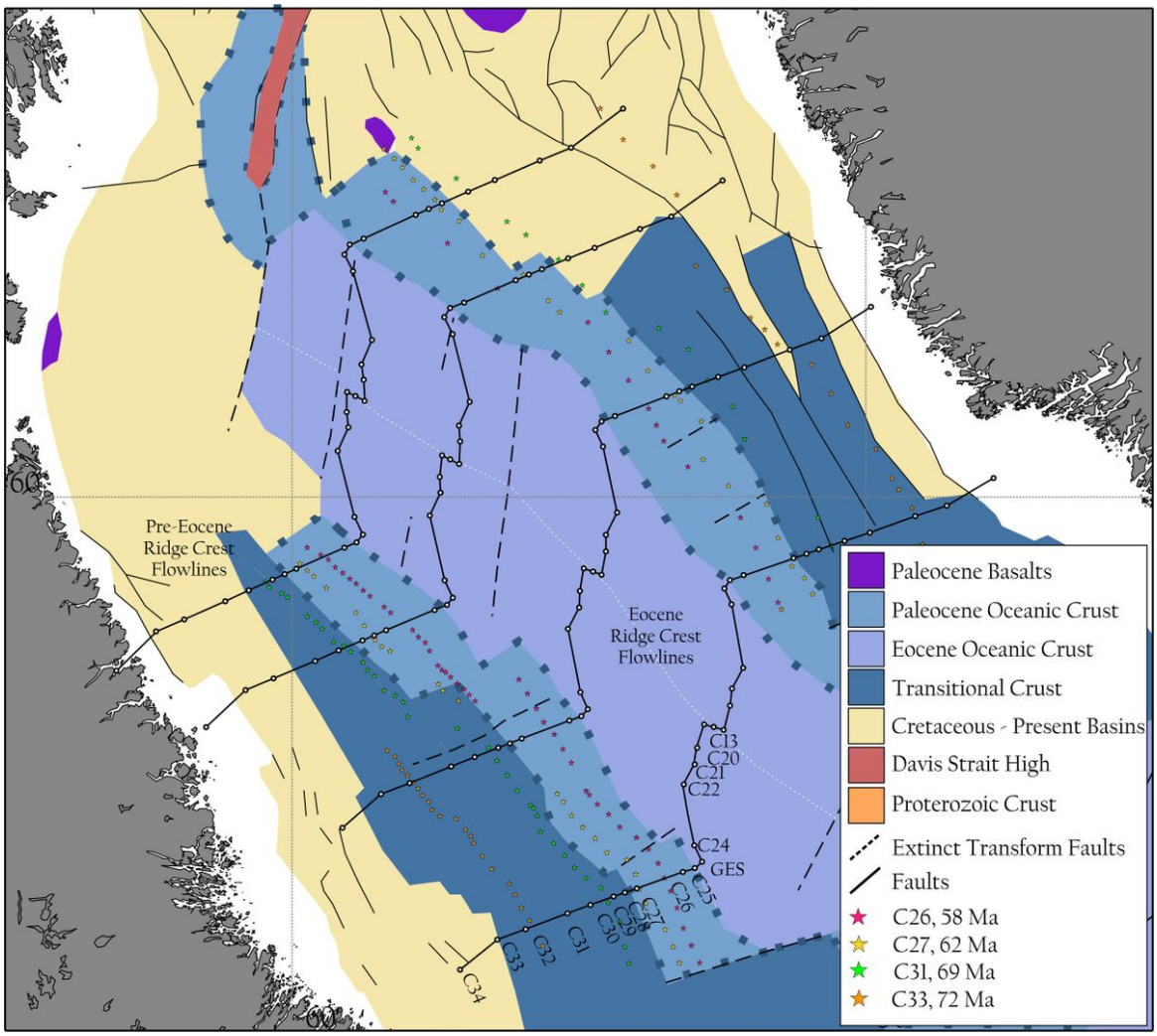

Figure 6

Plot of ridge crest flowlines in the Labrador Sea from the Greenland and North America plate model (times after GES) and from the North America and Eurasia plate model plotted for the Greenland and North American plates before GES. Flow points interpolated for C26, C27, C28, C29, C30 and C32 by assuming constant spreading rates in the relevant periods, see Table 1A, Appendix A. Magnetic isochron picks C33, C31, C27, C26, C25, C24 GSFML; 37 and C22, C21 71. Fracture zones picked from gravity data of 35. Paleocene – Eocene crustal boundary modified from 2 according to findings of this study, crustal shapes from 2.

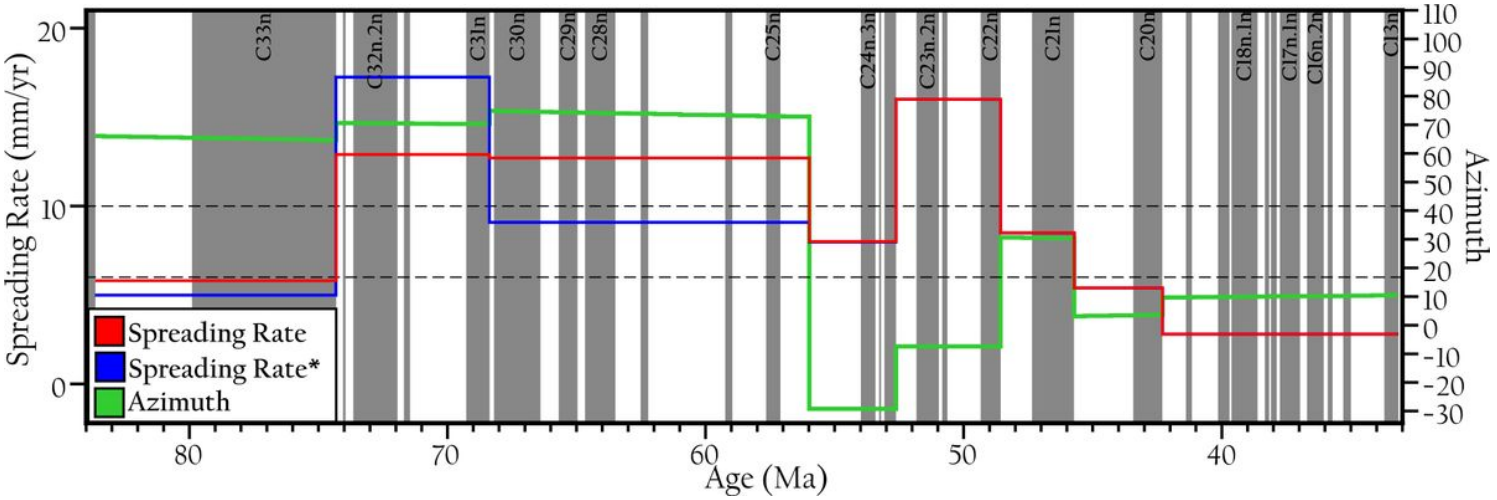

Figure 7

Spreading rates and azimuths (degrees clockwise from north) in the Labrador Sea, using the timescale of Gradstein et al., (2012)70. Spreading rates* correspond to those calculated using the interpolated GES rotation, assuming Greenland and Eurasia separated at 55.9 Ma.

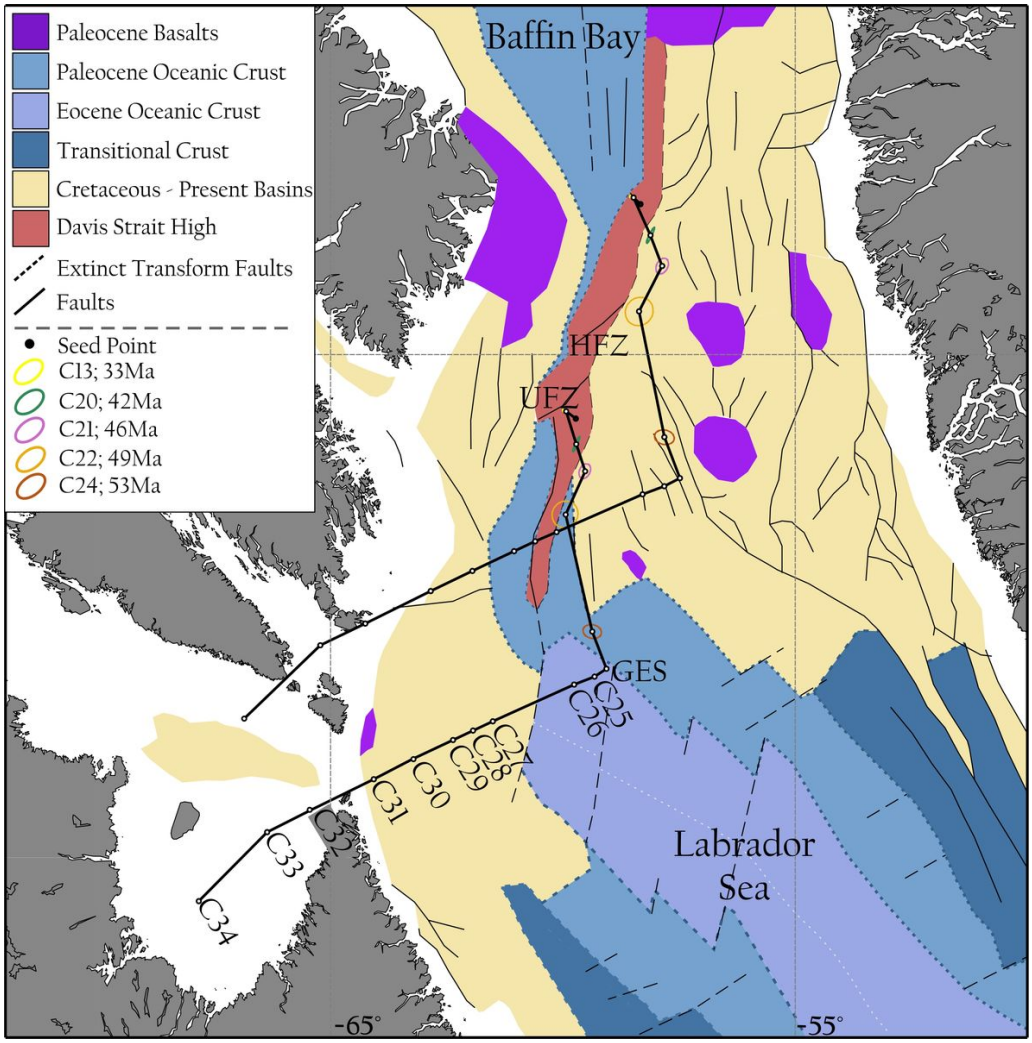

Figure 8

Whole-plate flowlines in the Davis Strait from the Greenland and North America plate model (C13 to GES) and Pre-Eocene ridge crest flowlines (C25 to C34) from the North America and Eurasia plate model, with their respective 95% confidence ellipses. Crustal shapes from 2.

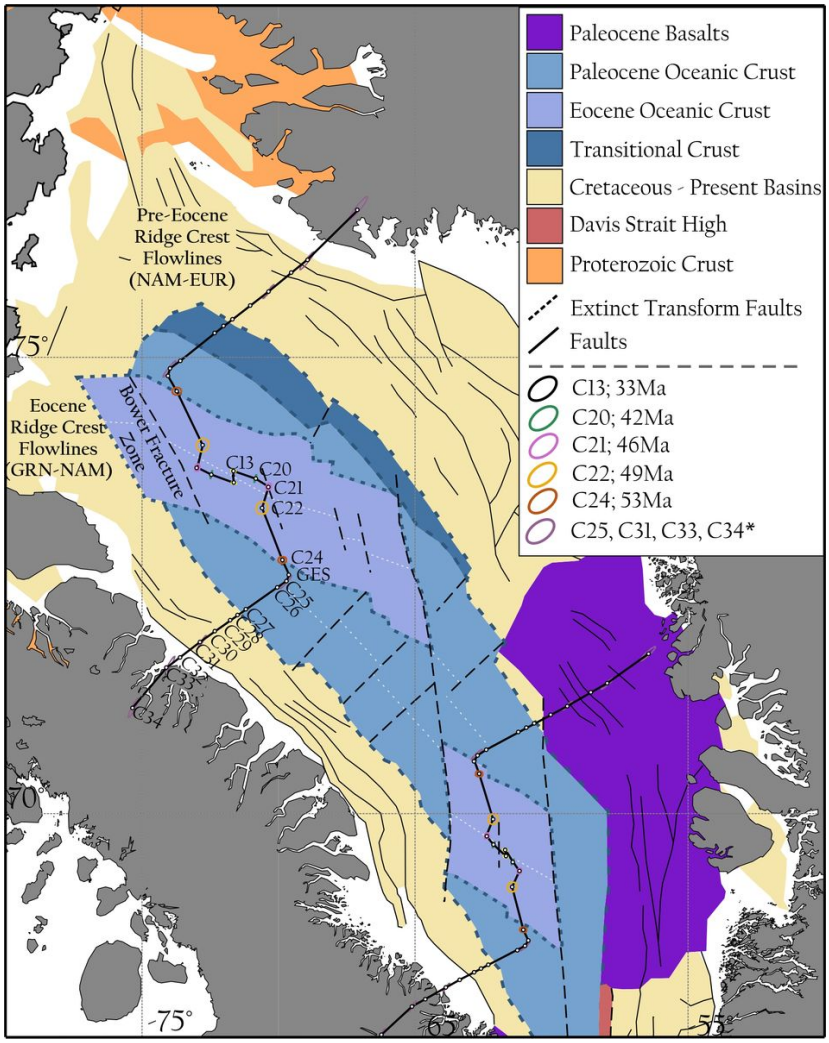

Figure 9

Plot of ridge crest flowlines in the Baffin Bay from the Greenland and North America plate model (C13 to GES) and Pre-Eocene ridge crest flowlines (C25 to C34) from the North America and Eurasia plate model, with their respective 95% confidence ellipses. Rotation for GES (-39.951/63.184/3.67) calculated assuming an age of 56 Ma. *Denotes ellipses derived from the North America and Eurasia plate model. Crustal shapes from 2.

Supplementary Files

This is a list of supplementary files associated with this preprint. Click to download.

- CodeDataset.7z
- GreenlandSupp.pdf